

Accurate physics-based modeling of electric vehicle energy consumption in the SUMO traffic microsimulator

Lucas Koch¹, Dominik S. Buse^{2,3}, Marius Wegener¹, Sven Schoenberg², Kevin Badalian¹, Falko Dressler³, and Jakob Andert¹

Abstract—Urban mobility is rapidly shifting toward electrification. Yet, limited range and availability of charging infrastructure will remain issues for Electric Vehicles (EVs) for the foreseeable future. Effectively managing these limitations for both individual vehicles as well as entire regions and cities requires accurate predictions of energy demand. Current tool chains such as Simulation of Urban Mobility (SUMO) already make use of simplistic energy consumption models. However, these models are often applicable only to specific vehicles and do not consider individual powertrain components’ characteristics. We close this gap and present a physics-based model for calculating energy consumption using component level modeling of the vehicle powertrain. The model is validated for EVs of different car segments against manufacturer data and test bench measurements. Through an open-source integration into SUMO, the model is available for public use. To showcase the possibilities of the proposed model and its flexibility, we perform a case study to predict the future energy demand of an exemplary mid-sized European city. The results show a strongly increasing demand for electric energy and underline the importance of considering heterogeneous vehicle fleets with different individual energy efficiency levels.

I. INTRODUCTION AND MOTIVATION

The ongoing electrification of vehicle powertrains represents a key technology on the road to sustainable mobility, especially in metropolitan areas [1]. To exploit the full environmental potential of vehicle electrification and achieve widespread acceptance of the technology, a demand-oriented infrastructure design is required that mitigates the disadvantages of the limited driving range and long charging duration. Therefore, energy consumption has to be considered very carefully both on the individual vehicle level and on city-scale. Microscopic traffic simulations, such as Simulation of Urban Mobility (SUMO), are particularly suitable for this type of analysis as they provide information down to the level of individual vehicles. Despite entailing considerable effort to generate realistic traffic scenarios (cf.[2]), the availability

of detailed information about trips and trajectories for every simulated road user provides a decent basis to estimate the individual vehicles’ energy consumption as well as network-wide demands. However, existing Electric Vehicle (EV) energy consumption models for microsimulators are often highly simplified, applicable only to specific vehicles, and do not consider the characteristics of individual powertrain components. As a results, they may lead to unrealistic energy consumption.

We thus propose a computationally efficient model for EV energy consumption calculation that is described in Section III. Its component-based design allows a simple but accurate estimation of all relevant physical effects in an EV’s powertrain. To ensure the validity of the model, we validate it against a chassis dynamometer measurement and against manufacturer’s information of various EVs on the market.

Further, we integrated the model into SUMO to enable EV simulations of various scales and scenarios. It is available for public use on GitHub.¹ By using this implementation, vehicles can be equipped with an electric powertrain device that computes the electric energy consumption during the simulation. The model can also report invalid power or torque demands to validate the simulated driving behavior. As a whole, this enables users to perform large scale simulations with EVs and obtain fine-grained energy consumption data. The SUMO implementation as well as a detailed comparison to the existing SUMO model are depicted in Section IV.

Finally, to demonstrate a possible application of the proposed model, a case study is presented in Section V to evaluate the future energy demand of an exemplary mid-sized city with temporal and spatial resolution of consumption data. Additionally, the impact of different electrification rates and different scenarios for the market share of each vehicle segment is explored. This showcases the capabilities of the model to gain both aggregated city-scale and fine-grained energy consumption predictions.

In summary, our main contributions are as follows:

- we developed an accurate, adaptable and computationally inexpensive EV powertrain energy consumption model,
- we integrated the model into the SUMO simulator including five different vehicles validated on publicly available data, available on GitHub¹ and
- we analyzed the electric energy demand for EVs in an urban driving scenario for the years 2025 and 2030.

¹Teaching and Research Area for Mechatronics in Mobile Propulsion, RWTH Aachen University, Germany, {koch_luc,wegener_ma,badalian_k,andert_j}@vka.rwth-aachen.de

²Software Innovation Lab and the Department of Computer Science, Paderborn University, Germany, {buse,schoenberg}@ccs-labs.org

³School of Electrical Engineering and Computer Science, TU Berlin, Germany, dressler@ccs-labs.org

Research reported in this article was conducted in part in the context of the Hy-Nets4all project (Grant No. EFRE-0801698), supported by the European Regional Development Fund (ERDF). Moreover, the work was partially performed in the Center for Mobile Propulsion funded by the German Research Foundation and the German Council of Science and Humanities. The authors gratefully acknowledge the funding of this project by computing time provided by the Paderborn Center for Parallel Computing (PC²).

¹https://github.com/mechatronics-RWTH/sumo/tree/ev_powertrain_device

II. RELATED WORK

First introduced in 2001, SUMO has become one of the most commonly used open-source tools for microscopic traffic simulation. Since 2014, SUMO offers its own built-in model for energy consumption of EVs [3] which will be referred to as “SUMO’s model” from here on. It calculates battery energy based on the difference in the vehicle’s potential and kinetic energy within two time steps. It considers losses from driving resistances as well as auxiliary energy consumers, but disregards the physical powertrain behavior. Conversion of electrical energy of the battery into mechanical energy at the wheel and vice versa is simplified by assuming a constant efficiency for propulsion and recuperation respectively. Those limitations led to various extensions of the SUMO model and the development of more advanced models by other contributors. Firstly, an adjustment of the recuperation efficiency depending on the vehicle’s deceleration was proposed to model the brake balance between electric motor and mechanical brakes [4]. Another improvement was achieved in [5] by accounting for temperature-dependent effects on the energy loss through a linear balancing term for ambient temperature deviation. In [6] various existing models and a new one proposed by the authors were compared along multiple driving cycles and test scenarios using SUMO. However, the proposed model was neither integrated into SUMO nor its implementation released. It was used to produce results based on traces exported by SUMO. Most recently, the latest version of the SUMO model was reviewed based on one specific EV model concluding that the primary causes of inaccuracy are recuperation phases and losses caused by the auxiliary consumers [7].

The estimation of traffic-related electric energy demand as a main field of application for EV consumption models has become an active area of research, often providing a basis for studies on the charging infrastructure. Some contributions like [8] forgo explicit modeling of EVs’ energy consumption to predict future charging demands, but instead derive the demand from battery capacities of current EVs on the market and assume randomly distributed battery State of Charge (SOC) levels when arriving at a charging station. Another common approach for estimating city-wide energy demand is realized by considering a constant [9]–[11] or linear, speed-dependent [12] energy consumption per electrically driven distance. This obviously lacks in accuracy for any real-world driving pattern. Probably closest to our approach are the contributions by [13] and [14]. To evaluate large-scale energy consumption in Sweden and Singapore, respectively, speed and road gradient dependent, map-based consumption models for EVs are used along a mesoscopic traffic simulation with relatively low spatial resolution.

Overall, despite various modifications over time, the SUMO model still exhibits some inaccuracies, especially in recuperation phases, and neglects the individual powertrain characteristics of EVs with different vehicle sizes. This paper aims at overcoming this limitations by introducing a component-level EV powertrain model for SUMO. In

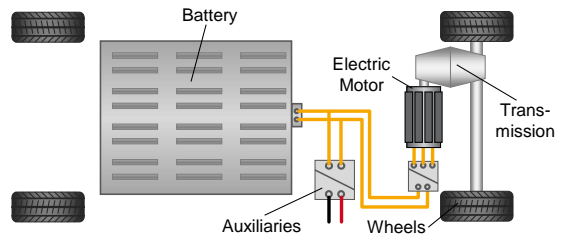


Fig. 1. Powertrain of a battery electric vehicle with rear-wheel drive.

combination with an urban traffic scenario, we show that this type of modeling can be a valuable tool for estimating energy demands on varying scales.

III. ENERGY CONSUMPTION MODEL FOR ELECTRIC VEHICLES

The following section covers the description and validation of the developed EV energy consumption model denoted as the “proposed model”.

A. Model Description

The powertrain of a battery electric vehicle usually consists of a high voltage battery, an electric machine with power electronics and a transmission as displayed in Figure 1. In addition, auxiliary energy consumers are to be considered. To enhance the accuracy of the energy consumption calculation in the traffic microsimulation, each powertrain component is modeled individually according to its unique efficiency characteristics. Further, modeling components individually opens up the possibility to adapt the model quickly to EVs of varying powertrain sizing. The proposed model is implemented as a backward calculation model that determines the components’ operating points and losses based on the required traction forces for the observed vehicle motion. This way of modeling does not allow for accurate calculations at power and traction limits since the causality of the motion is not considered, but enables the detection of unrealistic driving maneuvers that exceed the motor’s physical boundaries.

The necessary driving force F_W at the wheel is calculated based on the vehicles velocity v and acceleration a and its driving resistance parameters (see Equation (1)). The force to overcome a slope α is calculated using the product of vehicle mass m , gravitational constant g and the sine of the slope α . The rolling friction is modeled using the product of vehicle mass m , gravitational constant g , friction coefficient f_r and the cosine of α . Aerodynamic drag is calculated based on the air density ρ , drag coefficient c_w , vehicle frontal area A_f and the squared velocity v . The force to overcome the vehicles inertia is calculated from its mass m and acceleration a and corrected for the impact of rotational components in the powertrain using an equivalence factor e_i . The resulting torque at the wheels is the product of the driving force F_W and the effective radius of the wheel r_W .

$$F_W = mg \sin \alpha + mg f_r \cos \alpha + \frac{\rho}{2} c_w A_f v^2 + m e_i a \quad (1)$$

$$T_W = F_W \cdot r_W$$

The transmission includes a reduction gear as well as a differential gear-set resulting in an overall transmission ratio i_T from the electric motor shaft to the wheel. Its efficiency is assumed to be constant at η_T . The resulting mechanical torque at the electric motor T_{EM} is then calculated from the torque at the wheel T_W according to Equation (2).

$$T_{EM} = \begin{cases} T_W \cdot i_T^{-1} \cdot \eta_T^{-1} & \forall T_W \geq 0 \\ \max(T_W, T_{W,min}) \cdot i_T^{-1} \cdot \eta_T & \forall T_W < 0 \end{cases} \quad (2)$$

The minimum (negative) powertrain torque provided to the wheels $T_{W,min}$ is determined according to the (negative) torque limit $T_{EM,min}$ and (negative) power $P_{EM,min}$ limit of the electric motor and the transmission ratio and efficiency. Any additional braking torque to reach the overall required torque at the wheels T_W needs to be provided by the mechanical braking system.

$$T_{W,min} = \max\left(\frac{T_{EM,min} \cdot i_T}{\eta_T}, \frac{P_{EM,min} \cdot r_W}{\eta_T \cdot v}\right) \quad (3)$$

The efficiency characteristics of the electric motor are modeled using a two dimensional map that outputs the loss power $P_{EM,loss}$ based on the rotational speed n_{EM} and torque of the electric motor T_{EM} .

$$\begin{aligned} P_{EM,el} &= P_{EM,mech} + P_{EM,Loss} \\ P_{EM,loss} &= f(n_{EM}, T_{EM}) \end{aligned} \quad (4)$$

Apart from the driving resistances, the electric motor losses are the main impacting factor on the overall energy consumption. The majority of these losses scale non-linearly with the size of the motor, and any changes in the model parameters, except for the ones related to the battery, result in different motor operating points. While most model parameters can be obtained from openly available sources like sales brochures or datasheets, power loss maps are generally unavailable. To generate customized power loss maps for different vehicles with individual motor specifications nevertheless, the motor design tool developed in [15] is utilized. Given a set of motor parameters, it calculates power loss maps based on the physical effects inside the motor. Note that the motor design tool is designed only for Permanent-Magnet Synchronous Motors (PMSMs), so only EVs with this type of machine are considered in this study, although the powertrain model itself is not restricted to a specific motor type. Additional losses in the power electronics converting direct current to alternating currents and vice-versa are subsequently applied to the map by assuming a constant efficiency of 97%. Figure 2 shows the resulting power loss map modeled to match the specifications of the BMW i3. It can be observed that motor losses are increasing non-linearly with speed and absolute torque. The red lines at the respective maximum of the first and fourth quadrants represent the torque limits of the motor. Both minimum and maximum torque are assumed constant in the basic speed range until they reach their respective nominal speed. From there on, the field weakening restricts the motor torque under constant power. Both curves are determined

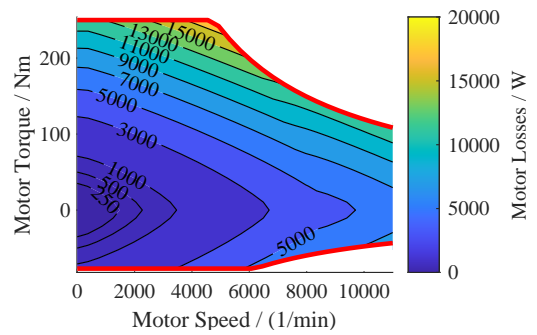


Fig. 2. Motor power loss map for the BMW i3 as modeled using [15].

TABLE I
ENERGY CONSUMPTION

Vehicle	Car Segment	WLTC Consumption in kWh/100 km		
		Manufacturer Data	Proposed Model	SUMO Model
VW e-up!	A	14.5–14.9	14.8	13.8
BMW i3	B	15.3–16.3	15.5	14.4
VW ID.3	C	15.4–15.9	15.9	15
VW ID.4	D	18.2–18.5	18.6	17.8
SUV	J	n.a.	23.7	22.1

by the parameters maximum (minimum) motor torque and power.

The electrical power at the battery is then calculated as the sum of the electrical power of the electric motor $P_{EM,el}$ and the auxiliary consumers' power $P_{aux,el}$ that is assumed to be constant for this study. The chemical power of the battery $P_{Bat,chem}$ is modeled using an internal resistance model with an open circuit voltage of U_0 and an internal resistance of R_i according to Equation (5).

$$\begin{aligned} P_{Bat,el} &= P_{EM,el} + P_{aux,el} \\ P_{Bat,chem} &= \frac{U_0^2}{2R_i} - U_0 \sqrt{\frac{U_0^2 - 4R_i P_{Bat,el}}{4R_i^2}} \end{aligned} \quad (5)$$

$P_{Bat,chem}$ represents the model output. By multiplication with the simulation step size, the energy consumption can be determined for the current time step.

B. Model Validation

Due to the generic structure of the proposed model, it can be adapted to any electric vehicle with the powertrain topology displayed in Figure 1 by adjusting the model parameters accordingly. To prove both scalability and accuracy, a two-stage validation process is applied. In the first step, we compare the results in the Worldwide harmonized Light vehicles Test Cycle (WLTC) for EVs from various car segments. To demonstrate the capability to reproduce the electrical battery power in a transient driving profile, the predicted battery power of the proposed model is compared against a test bench measurement in a second step.

For validation across a wide range of vehicle sizes, five EVs representative of different vehicle segments are simulated in the WLTC with the proposed model and compared to the manufacturer's type approval information (c.f., Table I). The

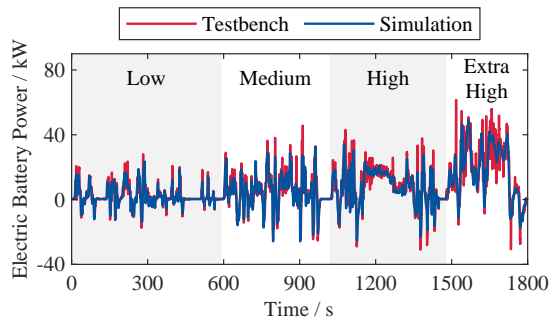


Fig. 3. Comparison of electric battery power in WLTC between the proposed model and a chassis dynamometer measurement.

same vehicles are also used for the case study in Section V. As an A-segment vehicle the VW e-up! was chosen, the BMW i3 is a B-segment vehicle, with the VW ID.3 and ID.4 representing the segments C and D, respectively. Since there is currently no J-segment vehicle in the EV market with a powertrain topology matching the modeled one (cf. Figure 1), an exemplary J-segment vehicle was parametrized based on an actual vehicle with slightly different topology from this segment. All model parameters used for this study can be found in Table II and will be analyzed further in Section IV. Since Worldwide harmonized Light vehicles Test Procedure (WLTP) specifications include losses that occur during battery charging (see [16]), all modeled energy consumption values are determined by applying an additional charging efficiency of 90% after the simulation. The results, including the energy consumption determined using SUMO's model, are listed in Table I. The range of energy consumption stated by the manufacturers can generally be reproduced accurately for each considered vehicle with the proposed model.

To rule out the possibility that only the accumulated battery power, but not its exact course correspond to the real behavior, an additional, more detailed analysis was conducted for the BMW i3 by measuring the real electrical power at the battery on a chassis dynamometer in the WLTC and comparing it with the simulated power consumption. Thereby, the measured electrical power at the battery terminal corresponds to the electrical battery power $P_{EM,el}$ in Equation (5). The resulting battery power in Figure 3 shows that all four WLTC segments are reproduced with high fidelity in transient driving mode. Notable deviations occur almost exclusively in short load peaks. Here, also the difference between the prescribed WLTC speed and the actual vehicle speed on the chassis dynamometer has to be considered. Especially in the extra high segment, the test bench driver has to readjust the accelerator pedal position constantly resulting in the fluctuating battery power of the testbench vehicle, while the simulated vehicle follows the specified speed without any deviation. Overall, the Root Mean Square Error (RMSE) over the entire cycle is 4.99 kW. Still, the cumulative battery power over the entire cycle deviates by only about 1%. Thus, it can be shown that not only the total results, but also the exact profile of the battery power is reproduced precisely with the proposed model.

IV. EV POWERTRAIN MODELING IN SUMO

To enable the use of the proposed model in simulation studies, we integrated it into SUMO. The model is available online for public use (see link on Page 1).

A. SUMO Integration

The proposed model is implemented as an (optional) *device* in SUMO. Vehicles in the simulation can be configured as EVs by providing the model parameters for its vehicle type (*vType*). The implemented device computes the electric power consumption in every time step. Further, it also checks the validity of the vehicle's driving state in order to detect operating points beyond the limits of the motor.

Individual vehicles or entire classes of them can be equipped with this EV powertrain device. This allows simulations with various EVs at the same time and preserves compatibility with many other SUMO features, e.g., vehicle type sampling, different driver models, elevation data, etc. Each vehicle type with an EV powertrain device can have the model parameters specified as vehicle type attributes. All computed quantities can be saved to an XML file as it is typical for SUMO. This file contains the model's input parameters (speed, acceleration, and slope) and the resulting chemical battery power as well as a validity indicator for each vehicle and time step. These results are gathered for all EV powertrain devices in the simulation, across all EV types.

While the proposed model is ready for simulation studies, some steps of further integration into SUMO still remain open. The data produced by the proposed model is currently not accessible via the SUMO GUI or TraCI. Also, due to the implementation as a backwards model, there is no coupling between the proposed model and the driver models to limit the speed in order to avoid invalid states or the battery model to track the battery SOC yet.

B. Comparison to SUMO Model

In the following, we highlight the main differences between the proposed model and SUMO's model and analyze the impact on the resulting energy consumption. There are four major features that sets the proposed model apart from the SUMO model. The proposed model

- contains individual models for all powertrain components,
- uses a characteristic map to derive speed and torque dependent motor power losses,
- limits the energy that can be recuperated through regenerative braking and
- detects and reports invalid states if the torque, speed or power demand exceeds the motor limits.

For a seamless switching between the SUMO model and the proposed one, the configuration set of vehicle type attributes are compatible and have only been extended by additional parameters. A complete overview of all parameters from both models is given in Table II for the BMW i3 where all values originate from public sources only. Configuration files of all EVs considered in this paper (c.f. Table I) are available with the released model. Since the power demand

TABLE II
MODEL PARAMETERS OF BOTH MODELS FOR THE BMW i3

Model Parameter	Proposed Model	SUMO model
Vehicle Mass	1417 kg	1417 kg
Powertrain Inertia	12.5 kgm ²	12.5 kgm ²
Roll Drag Coefficient	0.007	0.007
Radial Drag Coefficient	-	0
Front Surface Area	2.38 m ²	2.38 m ²
Air Drag Coefficient	0.29	0.29
Wheel Radius	0.3498 m	-
Propulsion Efficiency	-	82 %
Recuperation Efficiency	-	82 %
Gearbox Efficiency	96 %	-
Gear Ratio	9.665	-
Max. Motor Propulsion Power	125 000 W	125 000 W
Max. Motor Propulsion Torque	250 Nm	-
Max. Motor Recuperation Power	50 000 W	-
Max. Motor Recuperation Torque	77 Nm	-
Power Loss Map	$f(\eta_{EM}, T_{EM})$	-
Auxiliary Consumers' Power	360 W	360 W
Battery Capacity	-	39 000 Wh
Internal Battery Resistance	0.0768 Ω	-
Nominal Battery Voltage	370 V	-
Stopping Threshold	-	0.1 km/h

from the driving resistances is calculated in the same way, the associated parameters coincide. However, the SUMO model only uses two constant efficiencies to describe the conversion from mechanical wheel power to chemical battery power and vice versa, while the proposed model requires the parameters of all powertrain components. Among these, the characteristic power loss map (see Figure 2) is the most elaborate one. As mentioned in Section III, it is generated with the motor design tool [15]. The resulting *MATLAB* array is then converted into a serialized array stored in the vehicle type attributes by executing the provided *convertMapMat2XML* script. In the simulation, the map gets sampled for the closest point available to interpolate the instantaneous motor power loss. The maximum (minimum) motor power and torque enable the limitation and validation of the motor's operating point.

For the comparison of model accuracy, both models are executed in SUMO with the same BMW i3 parametrization, where applicable (cf. Table II). To achieve comparable results, the propulsion and recuperation efficiencies of the SUMO model need to be aligned with the components' efficiencies. While this is easily possible for the gearbox and inverter as they are represented by a constant efficiency themselves, the electric motor and battery efficiencies can only be estimated based on average values. In this way, the propulsion and recuperation efficiencies η_{Prop} and η_{Recu} for the comparison can be approximated.

$$\eta_{Prop} = \eta_{Recu} = \underbrace{96\%}_{\text{Gearbox}} \cdot \underbrace{90\%}_{\text{Motor}} \cdot \underbrace{97\%}_{\text{Inverter}} \cdot \underbrace{98\%}_{\text{Battery}} = 82\% \quad (6)$$

As the WLTC results in Table I indicate, the SUMO model generally underestimates the energy consumption, which is consistent with previous studies [7]. Overall, the resulting differences in energy consumption amount to 4–7 % depending on the vehicle. Since the calculation of driving resistances as well as the gearbox and inverter efficiencies coincide in both

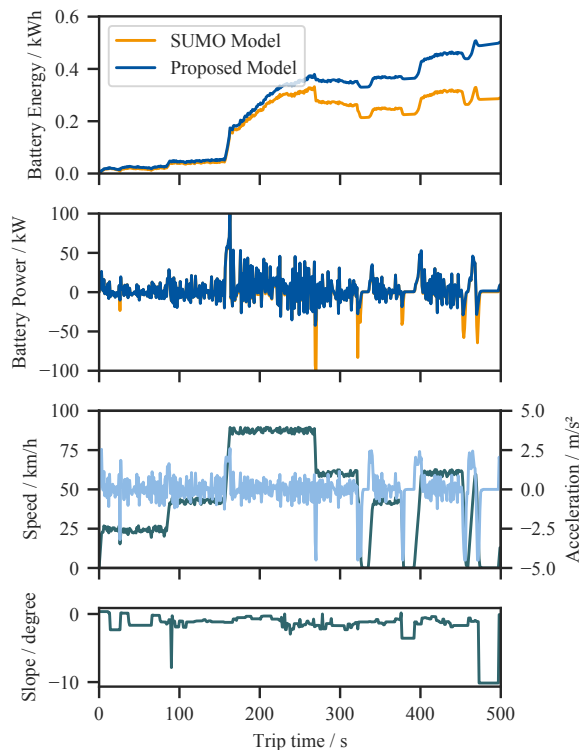


Fig. 4. Comparison of battery power for on an exemplary trip between the proposed model and the SUMO model for a BMW i3.

models, the gain in accuracy can be exclusively attributed to the motor's and battery's operating point-dependent efficiency and the limited recuperation capability.

For an in-depth investigation of those two effects under more realistic urban conditions, a representative driving sequence (see Figure 4) is selected from the trips for the case study performed in Section V and executed with both models. In contrast to the WLTC, this sequence contains more aggressive acceleration and deceleration phases, a noisy acceleration signal and a varying downward slope. The comparison of the instantaneous battery power reveals that the difference between the models can be significantly higher under more realistic conditions. For the considered 500 s sequence, the energy consumption predicted by the proposed model is 1.73 times higher than the result from the SUMO model. Those deviations result both from the limited recuperation capability in acceleration peaks and from shifted load peaks under nearly constant speed and slope. The changes in motor efficiency due to the shifted load points are particularly pronounced when the motor is operated at low speed and torque. The downward slope further leads to a lower motor torque and thus less efficient motor operation. Both results in a small but consistent underestimation of battery power illustrated by the constantly diverging battery energy in the upper diagram of Figure 4. High deviations, on the other hand, appear during strong deceleration phases where the motor's torque and power constraints limit the battery power. In these situations, as it is the case in the real vehicle, the proposed model caps the recoverable energy, while the

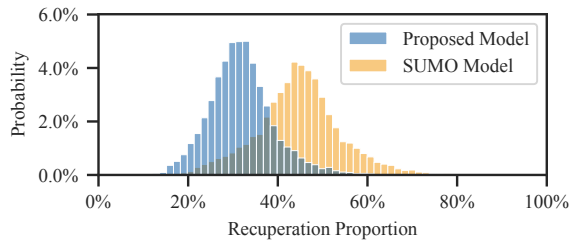


Fig. 5. Distribution of the proportion of recuperated energy to total energy per trip.

SUMO model feeds all the energy back into the battery. Those high deviations in the recuperated battery energy occur less frequently compared to the consistent underestimation of the motor efficiency, but has a greater impact on the final energy consumption (cf. the second diagram in Figure 4).

For further evaluation of the recuperation phases and the advantages of the introduced motor limits, we analyze all trips from the case study in Section V and compare the total proportion of recuperated to consumed battery energy during the trip. The resulting distributions for the proposed model (blue) and the SUMO model (orange) are shown in Figure 5.

In [6] proportions of recuperated energy of 7–31%, strongly depending on the considered driving cycle, are reported in simulation with a detailed energy consumption model. Since the trips considered in Figure 5 contain lots of stop-and-go maneuvers, the share of recuperated energy tends to be generally higher. However, the proposed model is still close to the expected range with an average recuperation proportion of 32%, whereas the majority of trips conducted with the SUMO model (average proportion of 45%) exceed this range by far. In addition to the overall lower amount of recuperated energy, Figure 5 also illustrates a wider range of recuperation proportions for the SUMO model.

In terms of computation performance we could not detect a significant difference in runtime between the models. In the case study, the difference was less than 1% on average.

V. CASE STUDY

In the following, we utilize the implementation of the proposed model in SUMO for a large-scale case study. The goal is to predict the current and future electric energy demand caused by passenger cars in Paderborn, Germany. We simulated the traffic of a regular weekday with an increasing EV share to model the evolution of traffic electrification in the coming years. We further considered three scenarios of varying market shares of different EV segments.

The simulation study utilizes the Paderborn traffic simulation scenario [17]. It models the city of Paderborn, a typical mid-sized European city with around 150 000 inhabitants. The scenario contains the core of the city as well as outskirts (cf. Figure 9). Road types include major highways, arterial roads and urban streets, down to residential and industrial areas, all augmented with elevation data. The scenario comes with a traffic demand data set of more than 200 000 trips over a 24 hour period with up to 3000 simultaneously active

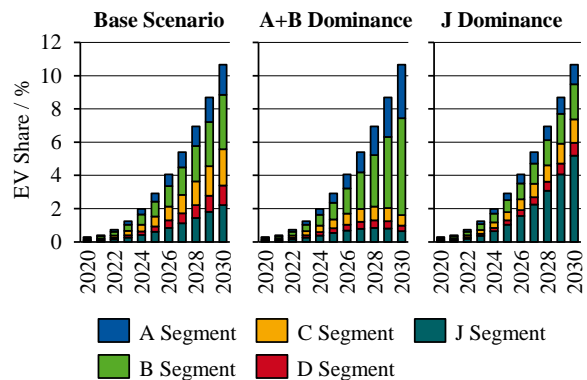


Fig. 6. Scenarios for varying EV distributions among the car segments.

TABLE III
ESTIMATED FUTURE EV SHARE

Year	EV Share in %		
	Min.	Mean	Max.
2020	0.29	0.29	0.29
2025	2.47	2.91	3.36
2030	9.15	10.66	12.16

vehicles. It resembles a typical day of the week, with the daily traffic demand curve resembling real-world measurements. Simulations were performed using SUMO version 1.6.0 (enhanced with our powertrain device), the default *Krauss* car following model and a step size of 1 s.

A. Traffic Electrification Scenarios

Traffic-related electric energy demands are primarily driven by the absolute number of electric vehicles on the streets. For this case study we obtained the predicted minimum and maximum number of EVs in Germany² to estimate the evolution of the EV shares in 2025 and 2030. The predicted EV shares are listed in Table III including the official data for 2020³. For the purpose of this study, it is assumed that the presented Germany-wide numbers also hold true for the city of Paderborn.

In addition to the absolute number of EVs, the future energy demand is also influenced by the distribution among the car segments. As Table I indicates, energy consumption per driven distance varies significantly between the different vehicle types. Since the general trend for EVs is still uncertain, three scenarios are considered for this study based on the five largest car segments by sales numbers among the EVs (A, B, C, D, J) and the actual distribution in Germany in 2020:

- Scenario 1 (Base): The distribution of car segments among the electric vehicles from 2020 remains constant until 2030.
- Scenario 2 (A+B Dominance): Mini and small vehicles (segments A and B) hold a dominant market share in the

²<https://www2.deloitte.com/de/de/pages/consumer-industrial-products/articles/elektromobilitaet-in-deutschland.html>

³https://www.kba.de/DE/Presse/Pressemitteilungen/2021/Allgemein/pm01_2021_E_Antrieb.html?nn=3033620

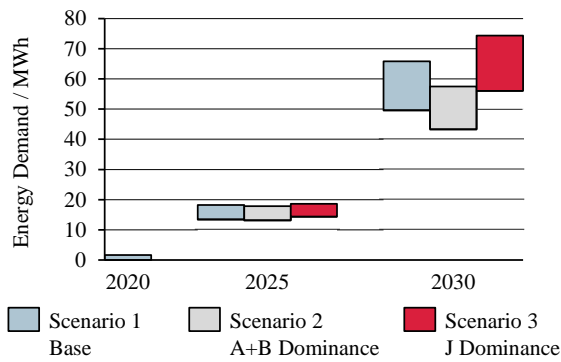


Fig. 7. Daily energy demand of electric passenger cars in Paderborn.

EV market in Germany compared to the entire vehicle fleet. For this scenario, a further growth of these two segments by 1% per year starting at a constant level with an equally proportioned decrease of the C, D and J segment is assumed.

- Scenario 3 (J Dominance): Since 2010, the overall market share of Sports Utility Vehicles (SUVs) (segment J) has increased by at least 13% per year⁴. In this scenario, it is assumed that this trend is also reflected in the EV market. Starting at an expansion rate of 13% per year, a constant decrease by 1% per year due to market saturation and an evenly distributed reduction of the four remaining segments is considered.

The three resulting distributions among the car segments are visualized in Figure 6 for the mean EV shares over the next 10 years from Table III.

B. Results

To estimate the future energy demand, simulations were conducted for all EV shares in Table III and each of the three distribution scenarios. For better comparability, we used the same trips for each of the simulation runs while randomly sampling EVs to the trips according to the respective penetration rate. To rule out distortions caused by adverse initialization, every combination was repeated 15 times with random seeds for SUMO (3 different seeds) and the assignments of EVs to the trips (5 different seeds). The proposed model has proven robust against these variations, with deviation of less than 1% in total energy demand. Furthermore, we observed a considerable number of cases where the SUMO driver model produced unrealistic driving states, especially on highway sections where motor torque was limited by the proposed model.

1) *Overall energy demand:* The estimated evolution of the total energy demand over time for the three studied scenarios is shown in Figure 7 where each bar represents the predicted range resulting from the minimum and maximum EV shares in Table III. As expected, a linear relationship between the city-wide energy demand and the number of electric vehicles is determined. The strong increase in energy demand between

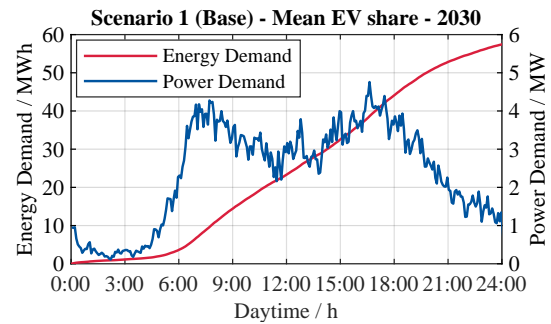


Fig. 8. Temporal distribution of electric passenger car related energy demand in Paderborn in 2030.

2025 and 2030 can thus be attributed to the rising number of EVs in this period. While the current electric energy demand of around 1.6 MWh is not yet significant, an average increase by a factor of 36 is expected until 2030. The resulting 57.7 MWh correspond to 7.2% of Paderborn's overall energy demand for a regular weekday in the summer of 2019, with charging losses not yet considered. However, depending on the development of EV sales and their distribution among the car segments, the expected urban energy demand varies by up to 30 MWh in 2030.

The effect of absolute EV penetration is significantly larger than the effect of varying vehicle segments, as can be seen from the figures for 2025. Due to the relatively small number of electric vehicles overall, the absolute impact of the various distributions on the vehicle segments is still minor. In 2030, however, the differences in the expected energy demand are already much more pronounced. A comparison between scenario 2 (A+B Dominance) and scenario 3 (J Dominance) with the mean EV market penetration yields a difference of 14.9 MWh. This corresponds to a fluctuation of 26% in relation to the mean value from the base scenario for the same distance traveled. In fact, all A and B segment vehicles in scenario 2 require nearly the same amount of energy as all SUVs in scenario 3. Despite only holding 49% of the total EV fleet, the J segment vehicles are responsible for 59% of the total energy demand.

2) *Temporal distribution of energy demand:* While results have always been aggregated for a whole day so far, the temporal resolution is crucial for an accurate demand analysis, for example as a first step to design an intelligent charging management. Figure 8 illustrates the course of power and cumulative energy demand over 24 hours for the base scenario with mean electrification rate in 2030, divided into five-minute segments. The power demand drops almost to zero in the middle of the night and then strongly increases to the first peak around 8:00 h mainly caused by commuters. After a slight decrease, the power demand stagnates at around 3 MW until it reaches its second, slightly higher peak at around 16:30 h. From this time on, the power demand decreases constantly while people drive back home and the majority of vehicles remain parked. Note that Figure 8 represents the actual consumption on the street that is not directly transferable, but temporally ahead of the power grid demand.

⁴https://www.kba.de/DE/Statistik/Fahrzeuge/Bestand/Segmente/b_segmente_inhalt.html?nn=2598042

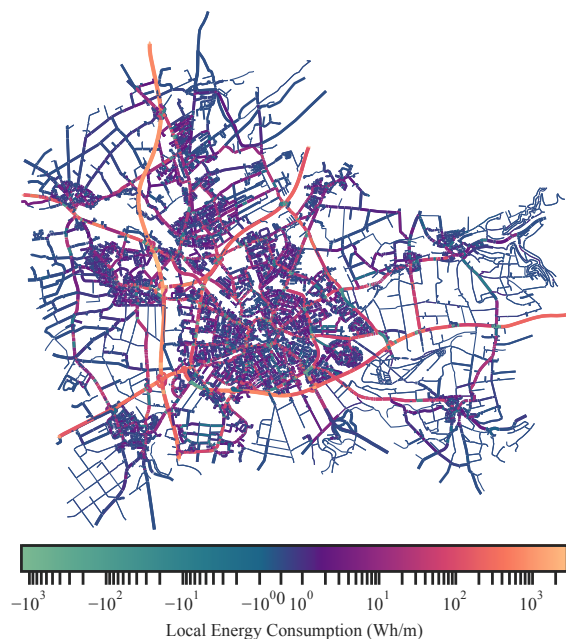


Fig. 9. Average local energy consumption of EVs in Paderborn in 2030. Indicates how much energy is consumed on which road by all EVs on one day, normalized to 1 m of road. Negative values due to downhill coasting.

3) *Spatial distribution of energy demand*: In addition to the city-wide energy consumption and time-dependent data the microscopic simulation can also provide insights on where EVs drive and thus where energy is spent. As shown in Figure 9, the highest local power consumption occurs on motorways and arterial roads. This appears plausible, as such roads typically experience higher amounts of traffic and average speed which lead to higher local energy consumption. On the other hand, Figure 9 also shows that certain roads have negative average power consumption per meter. These roads typically have a downhill slope or lead up to intersections towards which EVs slow down, both leading to the recuperation of energy.

VI. CONCLUSION AND OUTLOOK

In this paper, we have shown the need for accurate energy consumption modeling for EVs coupled with microscopic traffic simulation. To address this challenge, we presented a component-based powertrain model that estimates power loss at the electric motor using a characteristic map. While WLTC tests for vehicles from multiple car segments against manufacturer data proved general model validity, the accuracy was confirmed in a detailed comparison against a real vehicle measurement with an overall deviation in energy consumption of 1%. We further described the integration of this model into SUMO to allow flexible and large-scale simulations and released the model for public use. Then, we identified key issues with SUMO's EV energy consumption models, especially regarding over-estimated energy recuperation and neglected motor efficiency characteristics, and highlighted how the proposed model can improve the accuracy in these

cases. Finally, we showcased the applicability of the model in a case study that estimates the passenger car related energy of a mid-sized European city with increasing proportions of EVs and marked shares among EVs of different car segments.

Future work involves integrating the model into the next official SUMO release. We also target a deeper integration, e.g., regarding feedback of invalid states to the driver models and interaction with the battery device. Furthermore, we plan to utilize the model for energy-aware routing and public charging infrastructure design to prepare cities for the growing demand of EVs.

REFERENCES

- [1] United Nations, *Accelerating SDG 7 Achievement - Policy Brief 16 - Interlinkages between energy and transport*, 2018. [Online]. Available: <https://sustainabledevelopment.un.org/content/documents/17501PB16.pdf> (visited on 07/11/2021).
- [2] S. C. Lobo, S. Neumeier, E. M. G. Fernandez, and C. Facchi, "InTAS – The Ingolstadt Traffic Scenario for SUMO," arXiv, cs.NI 2011.11995, Nov. 2020. [Online]. Available: <https://arxiv.org/abs/2011.11995>.
- [3] T. Kurczveil and E. Schnieder, "Implementation of an Energy Model and a Charging Infrastructure in SUMO," in *SUMO User Conference 2013*, Berlin, Germany: Springer, May 2013, pp. 88–94.
- [4] C. Fiori, K. Ahn, and H. A. Rakha, "Power-based electric vehicle energy consumption model: Model development and validation," *Applied Energy*, vol. 168, pp. 257–268, Apr. 2010.
- [5] I. Sagaama, A. Kchiche, W. Trojet, and F. Kamoun, "Improving The Accuracy of The Energy Consumption Model for Electric Vehicle in SUMO Considering The Ambient Temperature Effects," in *IFIP/IEEE PEMWN 2018*, Toulouse, France, Sep. 2018.
- [6] B. Luin, S. Petelin, and F. Al-Mansour, "Microsimulation of electric vehicle energy consumption," *Elsevier Energy, Energy Scenario Toward 2030*, vol. 174, pp. 24–32, May 2019.
- [7] I. Sagaama, A. Kchiche, W. Trojet, and F. Kamoun, "Evaluation of the Energy Consumption Model Performance for Electric Vehicles in SUMO," in *IEEE/ACM DS-RT 2019*, Cosenza, Italy, Oct. 2019.
- [8] M. B. Arias, M. Kim, and S. Bae, "Prediction of electric vehicle charging-power demand in realistic urban traffic networks," *Applied Energy*, vol. 195, pp. 738–753, Jun. 2017.
- [9] H. Zhang, C. J. Sheppard, T. E. Lipman, T. Zeng, and S. J. Moura, "Charging infrastructure demands of shared-use autonomous electric vehicles in urban areas," *Transportation Research Part D: Transport and Environment*, vol. 78, Jan. 2020.
- [10] J. D. Kim and M. Rahimi, "Future energy loads for a large-scale adoption of electric vehicles in the city of Los Angeles: Impacts on greenhouse gas (GHG) emissions," *Energy Policy*, vol. 73, pp. 620–630, Oct. 2014.
- [11] B. Canizes, J. Soares, A. Costa, T. Pinto, F. Lezama, P. Novais, and Z. Vale, "Electric Vehicles' User Charging Behaviour Simulator for a Smart City," *Energies, Intelligent Transportation Systems for Electric Vehicles*, vol. 12, no. 8, Apr. 2019.
- [12] T. Hoché, D. Barth, T. Mautour, and W. Burghout, "Charging management of shared taxis: Neighbourhood search for the E-ADARP," in *IEEE ITSC 2020*, Ródos, Greece: IEEE, Sep. 2020.
- [13] F. J. Márquez-Fernández, J. Bischoff, G. Domingues-Olavarría, and M. Alaküla, "Using Multi-Agent Transport Simulations to Assess the Impact of EV Charging Infrastructure Deployment," in *2019 ITEC 2019*, Novi, MI: IEEE, Jun. 2019.
- [14] J. Ivanchev, J. Fonseca, and A. Knoll, "Electrification and Automation of Road Transport: Impact Analysis of Heat and Carbon Emissions for Singapore," in *IEEE ITSC 2020*, Ródos, Greece: IEEE, Sep. 2020.
- [15] S. Kalt, J. Erhard, and M. Lienkamp, "Electric Machine Design Tool for Permanent Magnet Synchronous Machines and Induction Machines," *Machines*, vol. 8, no. 1, 2020.
- [16] European Commission, *Commission Regulation (EU) 2017/1151*, 2017. [Online]. Available: <https://eur-lex.europa.eu/legal-content/EN/TXT/?uri=CELEX:02017R1151-20200125> (visited on 07/11/2021).
- [17] D. S. Buse, "Paderborn Traffic Scenario," Zenodo, Traffic Simulation Scenario version 0.1, Feb. 2021.